

# In Vitro Models of the Blood–Brain Barrier to Polar Permeants: Comparison of Transmonolayer Flux Measurements and Cell Uptake Kinetics Using Cultured Cerebral Capillary Endothelial Cells

MARK D. JOHNSON AND BRADLEY D. ANDERSON\*

Contribution from *Department of Pharmaceutics and Pharmaceutical Chemistry, University of Utah, Salt Lake City, Utah 84112.*

Received July 31, 1998. Final revised manuscript received December 31, 1998.  
Accepted for publication March 25, 1999.

**Abstract** □ Given that the cerebral microvasculature within the brain constitutes the rate-limiting barrier to drug entry, primary cultures of cerebral capillary endothelial cells would appear to offer a potentially useful model system for predicting drug delivery to the central nervous system. In the present study, the predictive capabilities of two potential models of the in vivo blood–brain barrier (BBB) to the passive diffusion of polar permeants were assessed. A comparison of the logarithms of the in vitro transmonolayer permeability coefficients ( $P_{\text{monolayer}}$ ) for several polar permeants varying in lipophilicity (from this study and literature data) with the well-established relationship between the logarithms of the in vivo BBB permeability coefficients ( $\log P_{\text{BBB}}$ ) and permeant lipophilicity as measured by the logarithm of the octanol/water partition coefficient ( $\log PC_{\text{octanol/water}}$ ) demonstrated that in vitro permeation across these monolayers is largely insensitive to polar permeant lipophilicity as a result of the predominance of the paracellular component in the transmonolayer flux. Conversely, kinetic studies of uptake of the same compounds into monolayers yielded transfer rate constants ( $k_p$ ) reflecting membrane permeability coefficients ranging over several orders of magnitude, similar to the variation in permeant lipophilicity. Furthermore, a linear relationship could be demonstrated between the logarithms of  $k_p$  and in vivo BBB  $\log P$  (slope =  $1.42 \pm 0.35$ ;  $r = 0.92$ ). In conclusion, this preliminary investigation suggests that monitoring the kinetics of cell uptake into cerebral capillary endothelial cell monolayers may be superior to transmonolayer flux measurements for predicting the passive diffusion of polar permeants across the BBB in vivo.

## Introduction

An in vitro model of the blood–brain barrier (BBB) that could mimic its in vivo barrier properties and thus allow one to predict the outcome of in vivo experiments would be extremely useful. Assuming the rate-limiting barrier to drug uptake to be the cerebral microvasculature, primary cultures of cerebral capillary endothelial cells offer a potentially useful model system for predicting drug delivery to the CNS.<sup>1,2</sup> Indeed, recent studies have led several investigators to conclude that primary cultures of cerebrovascular endothelial cells exhibit a barrier function that correlates with BBB function in vivo.<sup>3–5</sup> In vivo, the BBB permeability depends on permeant lipophilicity in a manner consistent with predominantly transcellular diffusion even for permeants as polar as sucrose, which has a log octanol/water partition coefficient ( $\log PC_{\text{octanol/water}}$ ) of approximately  $-4$ .<sup>6</sup> The present study confirms, however, that transmonolayer permeabilities across primary cultures

of BBB endothelial cells, a popular in vitro model of the BBB, fail to display the expected dependence on permeant lipophilicity for polar permeants having  $\log PC_{\text{octanol/water}} \leq 0$ . This paper therefore explores the utility of monolayer uptake kinetics as an alternative to transmonolayer flux measurements in an attempt to identify a more reliable model of the BBB for predicting permeability coefficients of polar permeants.

## Materials and Methods

**Reagents**—[ $^3\text{H}$ ]Sucrose (20 Ci/mmol) was obtained from NEN Research Products, DuPont, Wilmington, DE. [ $^{14}\text{C}$ (U)]Sucrose (600 mCi/mmol) and [ $^{14}\text{C}$ ]urea (59 mCi/mmol) were obtained from Moravak Biochemicals, Brea, CA. [ $^3\text{H}$ ]Mannitol (15 Ci/mmol), [ $^3\text{H}$ ]glycerol (30 Ci/mmol), and [ $^{14}\text{C}$ ]acetamide (55 mCi/mmol) were obtained from American Radiolabeled Chemicals Inc., St. Louis, MO. All radiolabeled compounds were purchased  $>98\%$  pure and were used without further purification. 3'-Azido-3'-deoxythymidine (zidovudine, 98% purity) was obtained from Aldrich Chemical Co., Milwaukee, WI. All other reagents were of analytical grade. Culture media consisted of minimum essential media (MEM)/F-12 Ham's nutrient mixture 1:1 (HyClone Laboratories, Logan, Utah) supplemented with 10 mM HEPES/13 mM sodium bicarbonate (pH 7.4), 100  $\mu\text{g}/\text{mL}$  penicillin G (Sigma Chemical Co., St. Louis, MO), 100  $\mu\text{g}/\text{mL}$  streptomycin (Sigma), 100  $\mu\text{g}/\text{mL}$  heparin (170 units/mg), and 10% plasma-derived horse serum (HyClone Laboratories).

**Isolation and Culture of Cerebrovascular Endothelial Cells**—Capillary segments were isolated from bovine cerebral gray matter (Dale T. Smith & Sons Meat Packing Company, Draper, UT) by a two-step enzymatic dispersion treatment followed by centrifugation over preestablished 50% Percoll density gradients as described previously.<sup>1</sup> Sequential filtering of the preparation through 500  $\mu\text{m}$  and 95  $\mu\text{m}$  nylon mesh filters yielded a relatively purified and homogeneous capillary suspension containing 5–20 individual endothelial cells per cluster. The isolated microvessels were cultured immediately or stored at  $-70^\circ\text{C}$  in culture medium to which had been added DMSO (10% v/v). Microvessels were seeded onto various surfaces at approximately 50 000 cells/cm<sup>2</sup> and cultured at  $37^\circ\text{C}$  under 95% humidity and 5% CO<sub>2</sub>/95% air. Culture media were changed every other day.

**Transmonolayer Flux Measurements**—Microvessels were seeded onto fibronectin-coated Biocoat (Becton Dickinson) cell culture inserts (fibrillar collagen matrix, 10.5 mm diameter,  $A = 0.9\text{ cm}^2$ , 1.0  $\mu\text{m}$  pore size,  $1.6 \times 10^6$  pores/cm<sup>2</sup>) and cultured as described above. Confluent monolayers were obtained within 9–10 days as determined visually via an inverted microscope. To provide clearance for a magnetic stir bar between the bottom of the plate well (six-well companion plate) and the microporous membrane of the insert, a 2 mm thick shim (60.0 mm diameter) was placed around the top of the well. Culture media (9.6 mL) was placed in the plate well (receiver chamber), and 0.9 mL was added to the insert (donor chamber) to maintain hydrodynamic stability. The system was allowed to equilibrate for 15 min at  $37^\circ\text{C}$  in an air incubator with continuous magnetic stirring. To initiate an experiment, the media in the insert was replaced with an equivalent volume of media containing [ $^3\text{H}$ ]– or [ $^{14}\text{C}$ ]–labeled and/or nonra-

\* To whom correspondence should be addressed. Tel: (801) 581-4688. FAX: (801) 585-3614. E-mail: banderson@deans.pharm.utah.edu.

diolabeled solute(s). At selected time points, samples (100  $\mu\text{L}$ ) were removed from the receiver chamber and immediately replaced with an equal volume of media. After the experiment, the donor concentration was analyzed to verify its constancy (i.e., >97% of initial concentration) throughout the experiment.

In some cases, transmonolayer flux measurements were also conducted using a vertical diffusion chamber system (Corning Costar Corp., Cambridge, MA) and Snapwell inserts (Corning Costar Corp.). Brain microvessels were seeded onto the cell culture inserts, which were thinly coated with rat tail collagen (type I) cross-linked with ammonia fumes<sup>2</sup> and cultured as described above. The two-piece cell culture devices consisted of 12 mm diameter, 0.4  $\mu\text{m}$  polycarbonate (10<sup>8</sup> pores/cm<sup>2</sup>) or polyester (10<sup>6</sup> pores/cm<sup>2</sup>) microporous membranes assembled in detachable rings. Confluent monolayers were typically obtained in 12–14 days, at which point the Snapwell insert ring was removed from the upper assembly and placed between the two halves of the diffusion chamber, thus minimizing cell monolayer disruption. Equal volumes (5 mL) of transendothelial assay buffer (122 mM NaCl, 25 mM NaHCO<sub>3</sub>, 10 mM D-glucose, 3 mM KCl, 1.2 mM MgSO<sub>4</sub>, 0.4 mM NaHPO<sub>4</sub>, 1.4 mM CaCl<sub>2</sub>, and 10 mM HEPES adjusted to pH 7.4 with NaOH)<sup>1</sup> were placed in both the donor (side facing the monolayer) and receiver sides. The chamber temperatures were maintained at 37 °C with a water-heated metal block. Both chambers were mixed using a 5% CO<sub>2</sub>/95% O<sub>2</sub> airlift. After 15 min of equilibration, the donor chamber was spiked with 0.5 mL buffer containing [<sup>3</sup>H]- or [<sup>14</sup>C]-labeled and/or nonradiolabeled solute(s). An equal volume of assay buffer was simultaneously added to the receiver chamber. Aliquots (100  $\mu\text{L}$ ) of the receiver solution were removed at various times along with equal volumes from the donor solution to maintain constant hydrostatic pressure.

Apparent permeability–area products ( $P_{\text{app}}A$ ) were obtained from the slopes of linear plots of permeant flux into the receiver compartment versus time,  $\Delta M_{\text{R}}/\Delta t$ , where  $\Delta M_{\text{R}} (= \Delta C_{\text{R}} V_{\text{R}})$  is the change in permeant mass over a given time interval,  $\Delta t$ , using the following relation:

$$P_{\text{app}}A = (\Delta M_{\text{R}}/\Delta t)/(C_{\text{D}} - C_{\text{R}}) \cong (\Delta C_{\text{R}} V_{\text{R}}/\Delta t)/C_{\text{D}} \quad (1)$$

where  $C_{\text{R}}$  was the concentration in the receiver and  $C_{\text{D}}$  was the donor concentration. Constant donor concentrations and sink conditions, respectively, were maintained (i.e.,  $C_{\text{D}} - C_{\text{R}} \approx C_{\text{D}}$ ) by ensuring that less than 10% mass transfer occurred over the time of the assay and by using large buffer volumes ( $V_{\text{R}}$ ) in the receiver chamber.

Monolayer permeability–area products,  $P_{\text{monolayer}}A$ , were determined from the following relationship:

$$1/P_{\text{app}}A = 1/P_{\text{monolayer}}A + 1/P_{\text{insert}}A \quad (2)$$

where permeability–area values for the collagen-coated insert ( $P_{\text{insert}}A$ ) were measured independently. Monolayer permeability coefficients,  $P_{\text{monolayer}}$ , were then obtained by dividing  $P_{\text{monolayer}}A$  by the surface area of the insert (i.e.,  $A = 0.9 \text{ cm}^2$ , Biocoat system;  $A = 1.13 \text{ cm}^2$ , Snapwell system).  $P_{\text{monolayer}}$  includes contributions from both paracellular and transcellular flux of solute across the cell monolayer (i.e.,  $P_{\text{monolayer}} = P_{\text{paracellular}} + P_{\text{transcellular}}$ ).

**Monolayer Uptake Experiments**—Rat tail collagen (type I) was attached to tissue culture dishes (35  $\times$  10 mm<sup>2</sup>) with a cross-linking reagent, 1-cyclohexyl-3-(2-morpholinoethyl)carbodiimide-metho-*p*-toluenesulfonate (Aldrich) to provide a uniform and durable surface for cell attachment and growth that would withstand multiple media changes and the wash procedure.<sup>7</sup> Brain microvessels were seeded onto the treated dishes, and confluent monolayers were obtained 8–10 days after initial plating. Uptake was initiated by the addition of fresh culture media containing [<sup>3</sup>H]- and/or [<sup>14</sup>C]-labeled or nonradiolabeled compounds (sucrose, mannitol, urea, and zidovudine at donor concentrations of  $1 \times 10^{-6}$ ,  $2.1 \times 10^{-7}$ ,  $5.1 \times 10^{-5}$ , and  $5.4 \times 10^{-3}$  M, respectively). At selected times, uptake was terminated by the rapid ( $\sim 1$  s) removal of uptake solution using a pipettor followed by a series of washes (50 mL per wash) with ice-cold Dulbecco's phosphate-buffered saline solution (pH 7.4). Dishes were immersed repeatedly (4 times) in wash solution and gently agitated (5 s per wash). (Validation experiments using urea and zidovudine detected no change in cellular content after the first wash.) Cells were solubilized with 1 N NaOH (15 min at room temperature) and

neutralized with an equivalent volume of 1 N HCl, and aliquots were analyzed for both permeant and protein content.

The mmoles solute per mg protein ( $M(t)$ ) in each monolayer versus time (one monolayer per time point) were recorded.  $M(t)$  includes potential contributions from both intracellular ( $M_{\text{monolayer}}(t)$ ) and any residual extracellular or surface bound permeant ( $M_i$ ) remaining after the washing procedure. Assuming that intracellular uptake is due to simple passive diffusion, the mass of permeant in the monolayer can be described by the following equation:

$$M(t) = M_{\text{monolayer}}(t) + M_i = C_{\text{D}} V_{\text{monolayer}}(1 - e^{-k_{\text{p}}t}) + M_i \quad (3)$$

where the monolayer volume per mg protein is  $V_{\text{monolayer}}$ ,  $k_{\text{p}}$  is the apparent first-order rate constant governing cell uptake ( $k_{\text{p}} = P_{\text{membrane}}A_{\text{monolayer}}/V_{\text{monolayer}}$ ), and  $C_{\text{D}}$  is the donor concentration of permeant. Experimental uptake versus time profiles were fit by nonlinear least-squares regression analysis to obtain estimates of  $V_{\text{monolayer}}$ ,  $k_{\text{p}}$ , and  $M_i$ .

Values of  $k_{\text{p}}$  for metabolizable compounds (i.e., glycerol and acetamide) were obtained from initial rates of cell uptake at glycerol donor concentrations of  $2.9 \times 10^{-7}$  and  $1.0 \times 10^{-3}$  M and acetamide donor concentrations of  $0.9 \times 10^{-6}$  to  $1.6 \times 10^{-5}$  M. Intracellular concentrations of permeant ( $C_{\text{monolayer}}(t)$ ) were calculated by dividing the intracellular mass (mmole/mg protein) by  $V_{\text{monolayer}}$  (7.2  $\mu\text{L}/\text{mg}$  protein, determined above from the nonmetabolized permeants). Plots of concentration vs time for these permeants were fit to eq 4 by linear least-squares regression

$$C_{\text{monolayer}}(t) = k_{\text{p}}C_{\text{D}}t + C_i \quad (4)$$

analysis to obtain the first-order rate constants for simple passive diffusion,  $k_{\text{p}}$ . Values of  $k_{\text{p}}$  for urea were also determined by this method over a concentration range of nearly 4 orders of magnitude ( $2 \times 10^{-5}$  to 0.1 M) to compare the two kinetic methods and to examine the concentration dependence of the cellular uptake of urea.

**Analytical Methods**—Samples containing [<sup>3</sup>H]- and/or [<sup>14</sup>C]-radionuclides were diluted with liquid scintillation cocktail (Opti-Fluor) and analyzed with a Beckman LS 1801 scintillation counter. Samples containing zidovudine were quantified with a modular reversed-phase HPLC system (Supelcosil LC-18-S analytical column) with UV detection at 254 nm. The mobile phase consisted of 15% acetonitrile in phosphate buffer (pH = 7.4,  $I = 0.02$ ). Protein content for each monolayer was determined by the Lowry method.<sup>8</sup>

**Statistical and Regression Analyses**—Statistical significance was determined using either a one-tailed or two-tailed Student's *t* test for unpaired data. Values were determined to be significantly different when  $P \leq 0.05$ . Nonlinear least-squares regression analysis was performed using a computer and commercially available software (SCIENTIST, MicroMath, Salt Lake City, UT).

## Results And Discussion

**Isolation and Culture of Cerebrovascular Endothelial Cells**—The isolation and culture of cerebral microvascular endothelial cells have led to the development of in vitro models designed to rapidly and conveniently examine various aspects of BBB function.<sup>2,9–11</sup> Primary cultures of these cells retain many characteristics of their cerebral counterparts, including specific BBB and endothelial “markers”, the absence of fenestrae, few micro-pinocytotic vesicles, an abundance of mitochondria, and well-developed junctional complexes.<sup>1,2,12–14</sup>

Bovine cerebral microvessels were isolated and characterized as described previously.<sup>15</sup> When seeded onto collagen-coated microporous surfaces, these cells showed excellent attachment and growth, with confluent monolayers forming within 8–10 days. Monolayers completely covered the insert, including along the edges, when examined microscopically and exhibited the characteristic spindle-shaped morphology described in the literature.<sup>1,13</sup> Furthermore, the permeability coefficients of polar permeants

Table 1—Physicochemical Properties and Permeability Coefficients (mean  $\pm$  SD) for the Transmonolayer Flux of Various Polar Solutes

permeant	MW	PC <sub>octanol/water</sub>	$P_{app}$ (cm/min $\times 10^3$ )	$P_{insert}$ (cm/min $\times 10^3$ )	$P_{monolayer}$ (cm/min $\times 10^3$ )	av log $P_{monolayer}$
sucrose	342	$2.1 \times 10^{-4}$ <sup>a</sup>	$1.70 \pm 0.46$ <sup>e</sup> $1.37 \pm 0.24$ <sup>f</sup> $1.09$ <sup>g,h</sup>	$2.29 \pm 0.05$ <sup>e</sup> $3.10$ <sup>f,h</sup> $5.98$ <sup>g,h</sup>	6.6 2.4 1.3	-2.56
mannitol	182	$3.4 \times 10^{-3}$ <sup>b</sup>	$1.50 \pm 0.27$ <sup>e</sup>	$3.03 \pm 0.46$ <sup>e</sup>	3.0	-2.52
glycerol	92	$1.1 \times 10^{-2}$ <sup>c</sup>	$3.59 \pm 0.97$ <sup>e</sup>	$5.01 \pm 0.18$ <sup>e</sup>	13	-1.9
urea	60	$2.6 \times 10^{-2}$ <sup>c</sup>	$3.47 \pm 0.51$ <sup>f</sup> $2.83$ <sup>g,h</sup>	$6.03$ <sup>f</sup> $10.56$ <sup>g,h</sup>	8.2 3.9	-2.25
acetamide	59	$8.9 \times 10^{-2}$ <sup>c</sup>	$3.31 \pm 0.31$ <sup>e</sup>	$4.82 \pm 0.59$ <sup>e</sup>	11	-1.96
zidovudine	267	$1.1$ <sup>d</sup>	$2.90 \pm 0.20$ <sup>e</sup> $3.92$ <sup>g,h</sup>	$3.84 \pm 0.26$ <sup>e</sup> $8.14$ <sup>g,h</sup>	12 7.6	-2.02

<sup>a</sup> Ref 32. <sup>b</sup> Ref 33. <sup>c</sup> Ref 34. <sup>d</sup> Ref 35. <sup>e</sup> Biocoat system ( $n = 3$  or  $4$  for  $P_{app}$ , except for zidovudine where  $n = 2$ ;  $n = 2$  for all  $P_{insert}$  values). <sup>f</sup> Vertical diffusion chamber system (Snapwell, polyester membrane);  $n = 3$  unless otherwise specified. <sup>g</sup> Vertical diffusion chamber system (Snapwell, polycarbonate membrane). <sup>h</sup> Single determinations.

frequently used as paracellular markers (e.g., sucrose and mannitol) were comparable to those reported in the literature.<sup>1,16,17</sup>

To establish that the in vitro culture system is a useful model system for predicting in vivo BBB permeability coefficients for passively diffusing polar permeants, it is essential that the in vitro model exhibit comparable barrier properties and similar selectivity to permeant structure (e.g., lipophilicity) as that observed in vivo. As demonstrated below, monolayers of cultured endothelial cells are too leaky and therefore provide neither the barrier properties nor the selectivity to polar permeant structure found in vivo.

**Transmonolayer Flux Measurements**—To evaluate the reliability of transmonolayer flux measurements for predicting in vivo brain uptake rates of passively diffusing polar permeants, several model permeants, listed in Table 1, were selected for transmonolayer experiments. The compounds chosen had molecular weights <400 daltons and varied in lipophilicity as measured by PC<sub>octanol/water</sub> by nearly 4 orders-of-magnitude. With the exception of zidovudine, the permeants employed, namely, sucrose, mannitol, glycerol, urea, and acetamide, have been used in numerous cerebrovascular permeability studies in vivo or in situ in which their transfer across the BBB was shown to occur via simple passive diffusion.<sup>18,19</sup> Zidovudine has also been shown to cross monolayers of bovine capillary endothelial cells primarily via passive diffusion,<sup>20</sup> although there is substantial evidence that its in vivo brain efflux is at least partially carrier-mediated.<sup>20–23</sup> Zidovudine's stability in endothelial cell homogenate made it a useful model permeant for this study, and its inclusion extended the range of lipophilicity explored, as measured by PC<sub>octanol/water</sub>, to 4 orders-of-magnitude ( $\sim 10^{-4}$  to 1).

Plots of % of permeant in the receiver compartment ( $100 \cdot C_R/C_D$ ) versus time for two representative permeants, mannitol and acetamide, in control (collagen-coated insert only) and transmonolayer flux experiments are shown in Figure 1. In all experiments, sink conditions were maintained, and consequently, linear profiles were observed, as demonstrated in Figure 1. As shown in Figure 1, fluxes across inserts containing monolayers were significantly ( $P \leq 0.05$ ) smaller than those across inserts without monolayers, indicating the presence of additional barrier function due to the monolayers. Least-squares regression analyses of the permeability data were performed to obtain permeability coefficients for the inserts ( $P_{insert}$ ) and for the monolayer/insert combinations ( $P_{app}$ ), as displayed in Table 1. Transmonolayer permeability coefficients ( $P_{monolayer}$ ), also shown in Table 1, were then obtained using eq 2 and the surface area of the insert.

log  $P_{monolayer}$  values generated in Table 1 are plotted in Figure 2 versus log PC<sub>octanol/water</sub> for each of the six per-

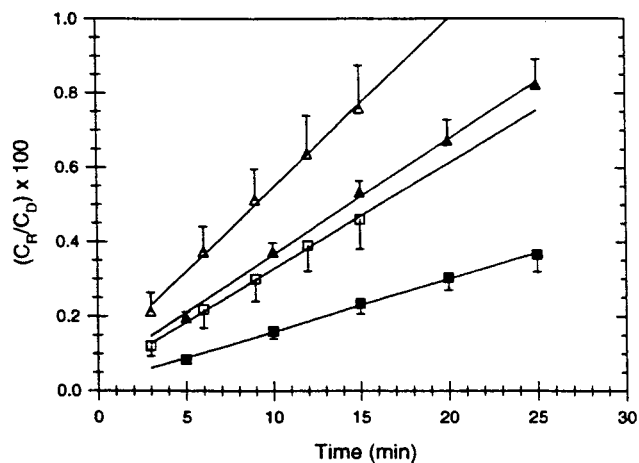


Figure 1—Representative transmonolayer flux ( $100 \cdot C_R/C_D$ ) profiles of mannitol (squares) and acetamide (triangles) across cell culture inserts with (filled symbols) and without (open symbols) confluent monolayers attached. Each time point represents the mean  $\pm$  SD of 2 or 3 individual experiments. The two solutes were present as a mixture. Donor concentrations of mannitol and acetamide were  $8.9 \times 10^{-8}$  and  $3.1 \times 10^{-5}$  M, respectively.

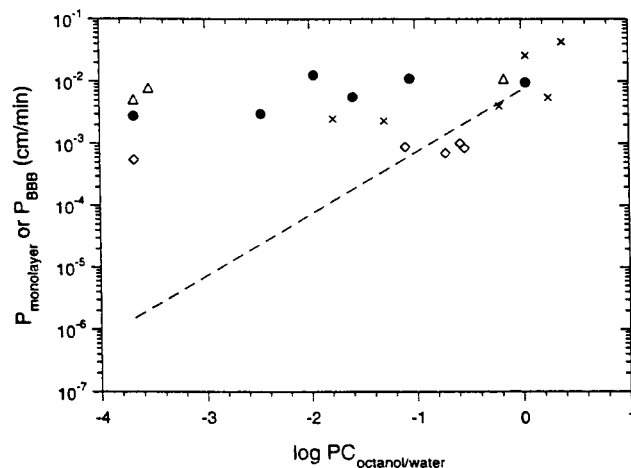


Figure 2—Semilogarithmic plots of  $P_{monolayer}$  versus log PC<sub>octanol/water</sub> for polar permeants having log PC values less than one. Results are from several laboratories, including this one (●); van Bree et al. (x);<sup>3</sup> Partridge et al. (Δ);<sup>4</sup> and Glynn and Yazdani (◇).<sup>24</sup> The dashed line is adapted from the literature regression line for BBB permeability–area product in vivo from Fenstermacher.<sup>6</sup>

meants. The dashed line in Figure 2 represents the in vivo relationship between the logarithm of the BBB permeability coefficient and log PC<sub>octanol/water</sub> according to eq 5,

$$\log P_{BBB} = -2.14 + \log PC_{octanol/water} \quad (5)$$

which was adapted from the regression line for the logarithm of BBB permeability–area product versus  $\log PC_{\text{octanol/water}} D_m$  published by Fenstermacher<sup>6</sup> by assuming a BBB surface area of 240 cm<sup>2</sup>/g of brain tissue and a permeant diffusion coefficient ( $D_m$ ) of  $1 \times 10^{-5}$  cm<sup>2</sup>/s. The literature regression line was based on *in vivo* BBB permeability data for a variety of permeants, including some from this study. It applies to approximately the same lipophilicity range as that covered in Table 1. As is evident in eq 5 and from the dashed line in Figure 2, the passive permeability of similarly sized polar permeants across the BBB *in vivo* appears to depend approximately linearly on  $PC_{\text{octanol/water}}$  (i.e., the slope of  $\log P_{\text{BBB}}$  versus  $\log PC_{\text{octanol/water}}$  is  $\sim 1$ ). This is the primary evidence for the conclusion by Fenstermacher<sup>6</sup> that passage across the BBB is transcellular, even for solutes as polar as sucrose. In stark contrast, the  $\log P_{\text{monolayer}}$  values exhibit virtually no dependence on  $\log PC_{\text{octanol/water}}$  within the range of lipophilicities explored, suggesting that the transmonolayer transfer of these solutes is mainly via a paracellular route (i.e., through leaks in the monolayer).

Because the extent of tight junction formation may vary with isolation technique, culturing conditions, etc., the results from several studies of the transmonolayer passage of low molecular weight permeants ( $\log PC_{\text{octanol/water}} < 1$ ) are also displayed in Figure 2, including data published by van Bree et al.,<sup>3</sup> Glynn and Yazdanian,<sup>24</sup> and Pardridge et al.<sup>4</sup> These data similarly show virtually no dependence of transmonolayer permeability on permeant lipophilicity for compounds having a  $\log PC_{\text{octanol/water}} < 1$ . Again, paracellular diffusion appears to predominate in these experiments.

Several investigators have observed that the barrier properties of endothelial cell monolayer cultures can be better maintained by coculturing with astrocytes<sup>25–27</sup> or with a combination of astrocyte-conditioned media and treatment with agents that elevate cyclic AMP.<sup>28</sup> Raub, for example, was able to demonstrate that noncontact coculture of postconfluent bovine brain cerebral capillary endothelial cell monolayers with rat C<sub>6</sub> glioma cells reduced  $P_{\text{monolayer}}$  for sucrose from  $1.47 \times 10^{-3}$  cm/min in primary cultures to  $7.7 \times 10^{-4}$  cm/min. An additional decrease to  $1.5 \times 10^{-4}$  cm/min was achieved with adenylate cyclase activators.<sup>27</sup> Dehouck et al. reported a sucrose permeability coefficient of  $6.3 \times 10^{-4}$  cm/min for monolayers in coculture.<sup>25,29</sup> These investigations indicate that some progress is evident in terms of improving barrier integrity by coculturing, but a comparison of these sucrose values with those shown in Figure 2 indicates that they are still orders-of-magnitude above the *in vivo* regression line.

**Monolayer Uptake Experiments**—Rate constants for permeant uptake into capillary endothelial cell monolayers ( $k_p$ ), which reflect the product of the membrane permeability coefficient,  $P_m$ , and monolayer surface-area-to-volume ratio (i.e.,  $k_p = P_m A_{\text{monolayer}} / V_{\text{monolayer}}$ ), were determined by measuring the accumulation of permeant in confluent monolayers after normalizing for the protein content in each monolayer.

Displayed in Figure 3 are plots of % uptake ( $100 \cdot M(t) / M_{\text{monolayer}(\infty)}$ ) versus time for the nonmetabolizable permeants sucrose, mannitol, urea, and zidovudine, along with the fitted curves obtained using eq 3. Independent estimates of monolayer volume, normalized to protein content, were obtained from each permeant as listed in Table 2. These estimates were not significantly different from each other as judged by their 95% confidence intervals and were therefore combined to give an average value of  $7.2 \pm 1.1$  (SEM)  $\mu\text{L}/\text{mg}$  protein, which, given an average protein

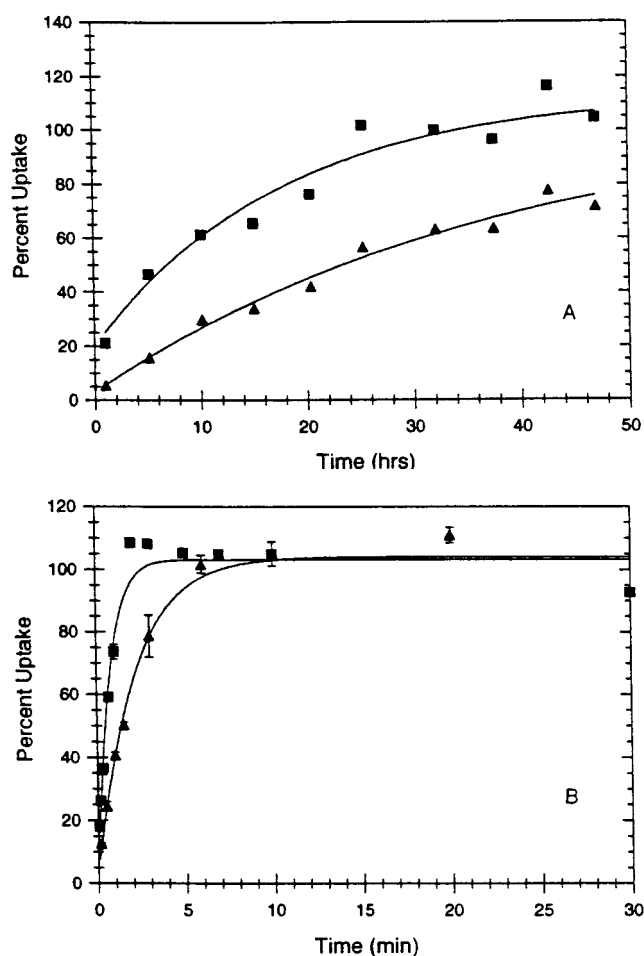


**Figure 3**—Percent uptake versus time profiles for (a) sucrose (▲) and mannitol (■) and (b) zidovudine (■) and urea (▲) into brain capillary endothelial cell monolayers. Each point represents an individual monolayer incubated at 37 °C for a given period of time in the presence of 1 mL of culture media containing  $1.0 \times 10^{-6}$  M sucrose,  $2.1 \times 10^{-7}$  M mannitol,  $5.4 \times 10^{-3}$  M zidovudine or  $5.0 \times 10^{-5}$  M urea, washed, and lysed for analysis. Values for urea (mean  $\pm$  SD) represent duplicate measurements at each time point.

**Table 2**—Parameters Obtained from Monolayer Uptake Experiments for Various Polar Permeants

permeant	$V_{\text{monolayer}}^a$ ( $\mu\text{L}/\text{mg}$ protein $\pm$ SD)	$k_p$ ( $\text{min}^{-1} \times 10^3 \pm$ SD)	$t_{1/2}$ (min)
sucrose	$7.2 \pm 1.1$	$0.45 \pm 0.05^a$	1540
mannitol	$7.9 \pm 0.8$	$0.85 \pm 0.27^a$	815
urea	$5.6 \pm 0.3$	$453 \pm 55^a$	1.6
glycerol	N/D	$373 \pm 13^b$ ( $n = 6$ )	4.5
acetamide	N/D	$155 \pm 7^b$ ( $n = 2$ )	1.1
zidovudine	$7.9 \pm 0.7$	$645 \pm 347^b$ ( $n = 3$ )	0.59

<sup>a</sup> Parameters determined from computer fits of the uptake versus time profiles to eq 3. <sup>b</sup> Parameters determined from computer fits of initial uptake rates to eq 4.

content of  $0.17 \pm 0.01$  (SEM) mg protein per monolayer corresponds to an intracellular volume in the monolayer of  $\sim 1.2 \mu\text{L}$ .

Intercepts in these plots reflect the residual percentage of permeant in cells at zero time due to extracellular or cell-surface-bound permeant remaining after the wash procedure. This residual percentage was  $< 5\%$  in all cases except for mannitol, where it was 18.5%. However, in every case, including that of mannitol, the residual percentage was not significantly different from zero as judged by the 95% confidence range.

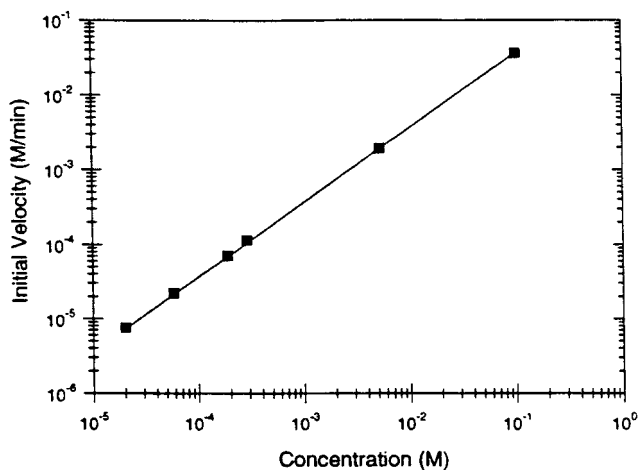


Figure 4—Dependence of initial rate of urea uptake into brain capillary endothelial cell monolayers on urea concentration. The solid line represents the fit using eq 4.

As evident in Figure 3a,b, concentrations of permeant in the monolayer appeared to reach equilibrium at distinctly different times. Zidovudine and urea attained apparent equilibrium within approximately 4 and 10 min, respectively, whereas the more hydrophilic molecules mannitol and sucrose took >24 h to approach a constant intracellular concentration. Indeed, the monolayer accumulation of sucrose had not yet achieved a steady-state concentration after 48 h when the study was terminated. In contrast to the similar  $P_{\text{monolayer}}$  values obtained in transmonolayer experiments, calculated values of  $k_p$  for each permeant obtained from these plots (Table 2) vary by >3 orders-of-magnitude from the slowest (sucrose) to the most rapidly permeating compound (zidovudine).

In addition to the % uptake versus time profiles in Figure 3a,b, initial rates of uptake were determined for urea over a concentration range of  $2 \times 10^{-5}$  to 0.1 M. Initial velocities were obtained from the slopes of plots of urea concentration in monolayers versus time as described by eq 4. These velocities, plotted versus urea concentration in Figure 4, demonstrate a linear relationship between rate of uptake and urea concentration consistent with uptake via passive (nonsaturable) diffusion. The first-order rate constant for urea uptake obtained from these data (Table 2) compared favorably with that obtained from the % uptake versus time profile in Figure 3b, thus validating the initial rate method for obtaining  $k_p$  values.

The initial rate method was employed to obtain  $k_p$  values for glycerol and acetamide after preliminary experiments suggested intracellular metabolism was occurring. Linear uptake kinetics were observed in the initial rate region for both permeants, consistent with eq 4, allowing the  $k_p$  values listed in Table 2 to be determined from linear least-squares regression analysis. The mean value for glycerol reflects initial rate studies conducted at concentrations of  $2.9 \times 10^{-7}$  and  $1.0 \times 10^{-3}$  M, which yielded  $k_p$  values of 0.16 and 0.15  $\text{min}^{-1}$ , indicating that uptake of glycerol was concentration-independent over this range.

All of the above results are consistent with a passive diffusion uptake mechanism. The adherence of the uptake curves in Figure 3a,b to a passive uptake model, the absence of concentration dependence in the initial rates of uptake of glycerol and urea, and the dramatic differences in  $k_p$  values, which qualitatively appear to be sensitive to permeant size and lipophilicity, support a passive diffusion mechanism. Estimates of monolayer volume were independent of the permeant employed to obtain the estimate for nonmetabolizable compounds, again consistent with passive diffusion.

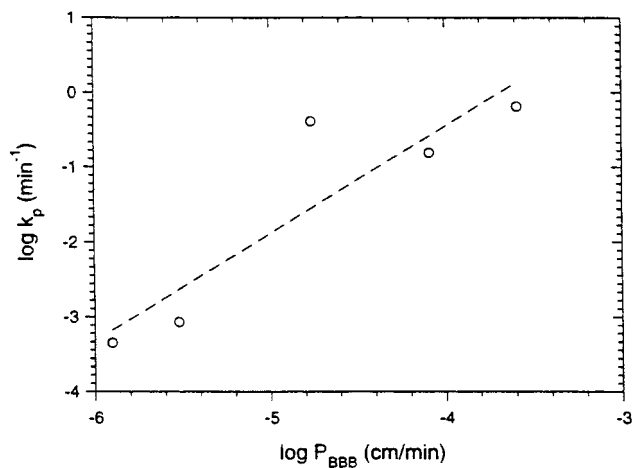


Figure 5—Relationship between  $\log k_p$  for uptake into brain capillary endothelial cell monolayers to  $\log P_{\text{BBB}}$  from published in vivo data.

The  $k_p$  values for monolayer uptake are related to the membrane permeability coefficient of each permeant ( $k_p = P_m A_{\text{monolayer}} / V_{\text{monolayer}}$ ). Therefore, these values would be expected to correlate with in vivo BBB permeability coefficients, provided that brain uptake in vivo is also passive for these permeants. Figure 5 displays the  $\log k_p$  values from this study plotted versus the average  $\log P_{\text{BBB}}$  values determined in vivo. The in vivo results for sucrose, mannitol, and urea were obtained from a compilation by Fenstermacher;<sup>6</sup> the glycerol value was the average of data from publications by Fenstermacher and Rapoport<sup>18</sup> and Takasato et al.;<sup>30</sup> and the acetamide literature value was from Rapoport et al.<sup>19</sup> Zidovudine was not included in this comparison because carrier-mediated processes have been implicated in its in vivo brain uptake/efflux.<sup>20,21,31</sup> The dashed line in Figure 5 represents the least-squares fit to the data, which yielded a slope not significantly different from one and an excellent correlation (slope =  $1.4 \pm 0.4$ ;  $r = 0.90$ ). There appears to be some size-dependent permeability behavior manifested more strongly in monolayer uptake than in vivo, as evident in the deviation of the  $k_p$  for urea, the smallest permeant examined, from the regression line. Why a larger size dependence would exist in the endothelial cell monolayers than in the cerebrovascular system in vivo is not known, if indeed it is the size of urea that accounts for the difference.

In conclusion, transmonolayer flux measurements appear to be poor predictors of blood-brain barrier passage in vivo for polar, small molecule permeants ( $\log PC_{\text{octanol/water}} < 0$ ), as transmonolayer permeability coefficients lack the sensitivity to permeant lipophilicity that is observed in vivo. This reflects the predominantly paracellular passage of polar permeants across brain endothelial cell monolayers. However, monolayer uptake kinetics of several polar permeants were found to be highly dependent on permeant lipophilicity and well correlated with in vivo BBB permeability coefficients, with a slope in the plot of  $\log k_p$  versus  $\log P_{\text{BBB}}$  near one. This preliminary investigation suggests that uptake studies into cerebral capillary endothelial cell monolayers may be superior to transmonolayer flux measurements for probing the role of simple passive diffusion in the passage of polar permeants across the blood-brain barrier. Additional studies are underway to assess the utility of the monolayer uptake method for predicting the in vivo BBB permeability of dideoxynucleoside anti-HIV agents which may also undergo intracellular metabolism during their passage across the BBB.<sup>15</sup>

## References and Notes

1. Audus, K. L.; Borchardt, R. T. Characterization of an in vitro blood-brain barrier model system for studying drug transport and metabolism. *Pharm. Res.* **1986**, *3*, 81-87.
2. Miller, D. W.; Audus, K. L.; Borchardt, R. T. Application of cultured endothelial cells of the brain microvasculature in the study of the blood-brain barrier. *J. Tissue Cult. Methods* **1992**, *14*, 217-224.
3. van Bree, J. B. M. M.; de Boer, A. G.; Danhof, M.; Ginsel, L. A.; Breimer, D. D. Characterization of an "in vitro" blood-brain barrier: Effects of molecular size and lipophilicity on cerebrovascular endothelial transport of drugs. *J. Pharmacol. Exp. Ther.* **1988**, *247*, 1233-1239.
4. Pardridge, W. M.; Triguero, D.; Yang, J.; Cancilla, P. A. Comparison of in vitro and in vivo models of drug transport through the blood-brain barrier. *J. Pharmacol. Exp. Ther.* **1990**, *253*, 884-891.
5. Shah, M. V.; Audus, K. L.; Borchardt, R. T. The application of bovine brain microvessel endothelial-cell monolayers grown onto polycarbonate membranes in vitro to estimate the potential permeability of solutes through the blood-brain barrier. *Pharm. Res.* **1989**, *6*, 624-627.
6. Fenstermacher, J. D. Pharmacology of the Blood-Brain Barrier. In *Implications of the Blood-Brain Barrier and Its Manipulation*; Neuwelt, E. A., Ed.; Plenum: New York, 1989; Vol. 1, pp 137-155.
7. Macklis, J. D.; Sidman, R. L.; Shine, H. D. Cross-linked collagen surface for cell culture that is stable, uniform, and optically superior to conventional surfaces. *In Vitro Cell. Dev. Biol.* **1985**, *21*, 189-194.
8. Lowry, O. H.; Rosebrough, N. J.; Farr, A. L.; Randall, R. J. Protein measurement with the folin phenol reagent. *J. Biol. Chem.* **1951**, *193*, 265-275.
9. Takakura, Y.; Audus, K. L.; Borchardt, R. T. Blood-brain barrier: Transport studies in isolated brain capillaries and in cultured brain endothelial cells. In *Advances in Pharmacology*; Academic Press: New York, 1991; Vol. 22, pp 137-165.
10. Audus, K. L.; Bartel, R. L.; Hidalgo, I. J.; Borchardt, R. T. The use of cultured epithelial and endothelial cells for drug transport and metabolism studies. *Pharm. Res.* **1990**, *7*, 435-451.
11. Joo, F. The blood-brain barrier in vitro: The second decade. *Neurochem. Int.* **1993**, *23*, 499-521.
12. Joo, F. The cerebral microvessels in culture, an update. *J. Neurochem.* **1992**, *58*, 1-17.
13. Bowman, P. D.; Betz, A. L.; Ar, D.; Wolinsky, J. S.; Penney, J. B.; Shivers, R. R.; Goldstein, G. W. Primary culture of capillary endothelium from rat brain. *In Vitro* **1981**, *17*, 353-362.
14. Williams, S. T.; Gillis, J. F.; Matthews, M. A.; Wagner, R. C.; Bitensky, M. W. Isolation and characterization of brain endothelial cells: morphology and enzyme activity. *J. Neurochem.* **1980**, *32*, 374-381.
15. Johnson, M. D.; Anderson, B. D. Localization of purine metabolizing enzymes in bovine brain microvessel endothelial cells: an enzymatic blood-brain barrier for dideoxynucleosides? *Pharm. Res.* **1996**, *13*, 1881-1886.
16. Pardridge, W. M. Brain metabolism: A perspective from the blood-brain barrier. *Physiol. Rev.* **1983**, *63*, 1481-1535.
17. Eddy, E. P.; Maleef, B. E.; Hart, T. K.; Smith, P. L. In vitro models to predict blood-brain barrier permeability. *Adv. Drug Delivery Rev.* **1997**, *23*, 185-198.
18. Fenstermacher, J. D.; Rapoport, S. I. Blood-brain barrier. In *Handbook of Physiology. Section 2: The Cardiovascular System. Vol IV: Microcirculation.*; Renkin, E. M., Michel, C. C., Eds.; American Physiological Society: Washington, DC, 1984; Vol. IV, pp 969-1000.
19. Rapoport, S. I.; Ohno, K.; Pettigrew, K. D. Drug entry into the brain. *Brain Res.* **1979**, *172*, 354-359.
20. Masereeuw, R.; Jaehde, U.; Langemeijer, M. W. E.; de Boer, A. G.; Breimer, D. D. In vitro and in vivo transport of zidovudine (AZT) across the blood-brain barrier and the effect of transport inhibitors. *Pharm. Res.* **1994**, *11*, 324-330.
21. Galinsky, R. E.; Hoestery, B. L.; Anderson, B. D. Brain and cerebrospinal fluid uptake of zidovudine (AZT) in rats after intravenous injection. *Life Sci.* **1990**, *47*, 781-788.
22. Collins, J. M.; Klecker, R. W., Jr.; Kelley, J. A.; Roth, J. S.; McCully, C. L.; Balis, F. M.; Poplack, D. G. Pyrimidine dideoxyribonucleosides: Selectivity of penetration into cerebrospinal fluid. *J. Pharmacol. Exp. Ther.* **1988**, *245*, 466-470.
23. Sawchuk, R. J.; Heydaya, M. A. Modeling the enhanced uptake of zidovudine (AZT) into the cerebrospinal fluid. 1. Effect of probenecid. *Pharm. Res.* **1990**, *7*, 332-338.
24. Glynn, S. L.; Yazdanian, M. In vitro blood-brain barrier permeability of nevirapine compared to other HIV antiretroviral agents. *J. Pharm. Sci.* **1998**, *87*, 306-310.
25. Dehouck, M. P.; Jolliet-Riant, P.; Bree, F.; Fruchart, J. C.; Cecchelli, R.; Tillement, J. P. Drug transfer across the blood-brain barrier: correlation between in vitro and in vivo models. *J. Neurochem.* **1992**, *58*, 1790-1797.
26. Dehouck, M.-P.; Meresse, S.; Delorme, P.; Fruchart, J.-C.; Cecchelli, R. An easier, reproducible, and mass-production method to study the blood-brain barrier in vitro. *J. Neurochem.* **1990**, *54*, 1798-1801.
27. Raub, T. J. Signal transduction and glial cell modulation of cultured brain microvessel endothelial cell tight junctions. *Am. J. Physiol.* **1996**, *271*, C495-C503.
28. Rubin, L. L.; Hall, D. E.; Porter, S.; Barbu, K.; Cannon, C.; Horner, H. C.; Janatpour, M.; Liaw, C. W.; Manning, K.; Morales, J.; Tanner, L. I.; Tomaselli, K. J.; Bard, F. A cell culture model of the blood-brain barrier. *J. Cell Biol.* **1991**, *115*, 1725-1735.
29. Chesne, C.; Dehouck, M. P.; Jolliet-Riant, P.; Bree, F.; Tillement, J. P.; Dehouck, B.; Fruchart, J. C.; Cecchelli, R. Drug transfer across the blood-brain barrier: comparison of in vitro and in vivo models. In *Frontiers in Cerebral Vascular Biology: Transport and Its Regulation*; Drewes, L. R., Betz, A. L., Eds.; Plenum Press: New York, 1993; pp 113-115.
30. Takasato, Y.; Rapoport, S. L.; Smith, Q. R. An in situ brain perfusion technique to study cerebrovascular transport in the rat. *Am. J. Physiol.* **1984**, *247*, H484-H493.
31. Takasawa, K.; Terasaki, T.; Suzuki, H.; Ooie, T.; Sugiyama, Y. Distributed model analysis of 3'-azido-2',3'-dideoxyinosine and 2',3'-dideoxyinosine distribution in brain tissue and cerebrospinal fluid. *J. Pharmacol. Exp. Ther.* **1997**, *282*, 1509-1517.
32. Levin, V. A. Relationship of octanol/water partition coefficient and molecular weight to rat brain capillary permeability. *J. Med. Chem.* **1980**, *23*, 682-684.
33. Barry, B. W.; Bennett, S. L. Effect of penetration enhancers on the permeation of mannitol, hydrocortisone and progesterone through human skin. *J. Pharm. Pharmacol.* **1987**, *39*, 535-546.
34. Wolosin, J. M.; Ginsburg, H.; Lieb, W. R.; Stein, W. D. Diffusion within egg lecithin bilayers resembles that within soft polymers. *J. Gen. Physiol.* **1978**, *71*, 93-100.
35. Barchi, J. J., Jr.; Marquez, V. E.; Driscoll, J. S.; Ford, H., Jr.; Mitsuya, H.; Shirasaka, T.; Aoki, S.; Kelley, J. A. Potential anti-AIDS drugs. Lipophilic, adenosine deaminase-activated prodrugs. *J. Med. Chem.* **1991**, *34*, 1647-1655.

## Acknowledgments

Support for these studies was provided by NIH Grant AI34133. Mark Johnson also received support as a recipient of an Advanced Predoctoral Fellowship in Pharmaceuticals from the Pharmaceutical Research and Manufacturers of America Foundation.

JS9803149